CDF note 8543

Search for the Rare Decays $B^+ \to \mu^+\mu^- K^+$, $B_d^0 \to \mu^+\mu^- K^{*0}$ and $B_s^0 \to \mu^+\mu^-\phi$

The CDF Collaboration
URL http://www-cdf.fnal.gov

(Dated: December 6, 2006)

We search for $b \to s\mu^+\mu^-$ transitions in exclusive decays of B mesons. Using $924\,\mathrm{pb}^{-1}$ of CDF Run II data, we find $\mathcal{B}(B^+ \to \mu^+\mu^- K^+) = (0.60 \pm 0.15 \pm 0.04) \times 10^{-6}$, $\mathcal{B}(B_d^0 \to \mu^+\mu^- K^{*0}) = (0.82 \pm 0.31 \pm 0.10) \times 10^{-6}$, and $\mathcal{B}(B_s^0 \to \mu^+\mu^-\phi)/\mathcal{B}(B_s^0 \to J/\psi\phi) < 2.61(2.30) \times 10^{-3}$ at 95(90)% CL. The measurements of the B^+ and B_d^0 modes are consistent with the world average and of similar precision as the best available measurements. The limit on $B_s^0 \to \mu^+\mu^-\phi$ is the most stringent to date.

Preliminary Results for Autumn 2006 Conferences

I. INTRODUCTION

The decay of a b quark into an s quark and two muons requires a flavor-changing neutral current (FCNC) process which is strongly suppressed in the standard model (SM). New physics models allow for significant deviations from the SM prediction [1–4].

While the $b \to s\gamma$ branching ratio has been accurately measured [5] and agrees with the theory predictions, the $b \to s\mu^+\mu^-$ transition allows the study of FCNC in more detail through additional observables, such as the dimuon invariant mass $m(\mu^+\mu^-)$, and the forward-backward asymmetry of the strange quark in the dimuon system.

The rare decays $B^+ \to \mu^+\mu^- K^+$ and $B^0_d \to \mu^+\mu^- K^{*0}$ have been observed at the B factories [6, 7]. However, searches for the analogous $B^0_s \to \mu^+\mu^-\phi$ decay, with a predicted branching ratio of 1.6×10^{-6} [10], did not reveal a significant signal [8, 9].

We search in $924\,\mathrm{pb}^{-1}$ of CDF Run II data for the rare decay modes $B \to \mu^+\mu^- h$, where B stands for B^+, B^0_d, or B^0_s, and h stands for K^+, K^{*0}, or ϕ respectively. The K^{*0} is reconstructed in the mode $K^{*0} \to K^+\pi^-$, and the ϕ is reconstructed as $\phi \to K^+K^-$. For normalization we use the abundant $B \to J/\psi h$ decays, which have final states identical to those of the rare decay modes, resulting in a cancellation of many systematic uncertainties in the ratio of branching ratios:

$$\frac{\mathcal{B}(B \to \mu^+\mu^- h)}{\mathcal{B}(B \to J/\psi h)} = \frac{N_{\mu^+\mu^- h}}{N_{J/\psi h}} \frac{\epsilon_{J/\psi h}}{\epsilon_{\mu^+\mu^- h}} \times \mathcal{B}(J/\psi \to \mu^+\mu^-), \tag{1}$$

where $N_{\mu^+\mu^- h}$ is the observed number of $B \to \mu^+\mu^- h$ decays, $N_{J/\psi h}$ is the observed number of $B \to J/\psi h$ decays, while $\epsilon_{J/\psi h}$ and $\epsilon_{\mu^+\mu^- h}$ are the selection efficiencies of $B \to J/\psi h$ and $B \to \mu^+\mu^- h$ respectively.

Throughout this text, charge conjugate modes are implicitly included.

II. THE CDF II DETECTOR

CDF II is a general-purpose particle detector, built with cylindrical symmetry around one of the two collision points of the Tevatron $p\bar{p}$ collider operating at a center-of-mass energy of $\sqrt{s} = 1.96\,\mathrm{TeV}$, and is described in detail elsewhere [11]. Charged particles are detected with the tracking system, immersed in a 1.4 T solenoidal magnetic field. A 7-layer silicon tracking system, ranging in radius from 1.5 to 28 cm, provides space-points of charged particle trajectories with an accuracy of approximately $15\,\mu$m. A proportional drift chamber provides up to 96 measurements of every charged particle trajectory from radii of 40 to 137 cm. A muon identification system is located outside the calorimeters. Four layers of planar drift chambers detect muons with a momentum transverse to the beamline, p_T, greater than 1.5 or $2.0\,\mathrm{GeV}/c$.

III. DATA SAMPLE & EVENT SELECTION

Signal candidates are selected online with a three-level trigger system. The first trigger level requires the presence of two charged particle trajectories with $p_T \geq 1.5\,\mathrm{GeV}/c$ or $2.0\,\mathrm{GeV}/c$, matched to activity in the muon chambers. At the second level, the trigger rate is reduced by requiring that the muons have opposite charge and that the opening angle in the projection transverse to the beamline is less than $120°$. At the third trigger level, the event is fully reconstructed and we select events where the muons are reconstructed in the silicon detector and their intersection has a transverse displacement from the beamline of at least $200\,\mu$m. The data sample used in this analysis corresponds to an integrated luminosity of $924\,\mathrm{pb}^{-1}$, collected from May 2003 to February 2006.

Candidates for the $B \to J/\psi h$ and $B \to \mu^+\mu^- h$ modes are selected by constructing a vertex of two muons that satisfy the trigger requirements with one reconstructed charged particle to form a $B^+ \to \mu^+\mu^- K^+$ candidate, or with two reconstructed particles of opposite charge to form a $B^0_d \to \mu^+\mu^- K^{*0}$ or $B^0_s \to \mu^+\mu^-\phi$ candidate. The χ^2 probability of the vertex fit is required to be 10^{-3} or better.

All charged particle trajectories are required to be observed in at least three layers of the silicon vertex detector and have $p_T \geq 0.4\,\mathrm{GeV}/c$. In addition, we require $p_T(h) \geq 1.0\,\mathrm{GeV}/c$ and $p_T(B) \geq 4\,\mathrm{GeV}/c$. A lower limit on the lifetime significance, $ct/\sigma_{ct} \geq 3$ and an upper limit on the impact parameter of the B candidate, $|d_0(B)| \leq 120\mu$m, help to reduce the background with little loss of signal.

For B^0_d candidates the $K^+\pi^-$ mass must lie within $50\,\mathrm{MeV}/c^2$ of the K^{*0} mass, and for B^0_s candidates the K^+K^- mass must lie within $10\,\mathrm{MeV}/c^2$ of the ϕ mass. No particle identification is used in the event selection. The ambiguity of the mass assignment in $B^0_d \to \mu^+\mu^- K^{*0}$ decays is handled by choosing the combination whose $K^+\pi^-$ mass is closest to the PDG value of the K^{*0} mass. This results in the right mass assignments for $\approx 90\%$ of the decays; the

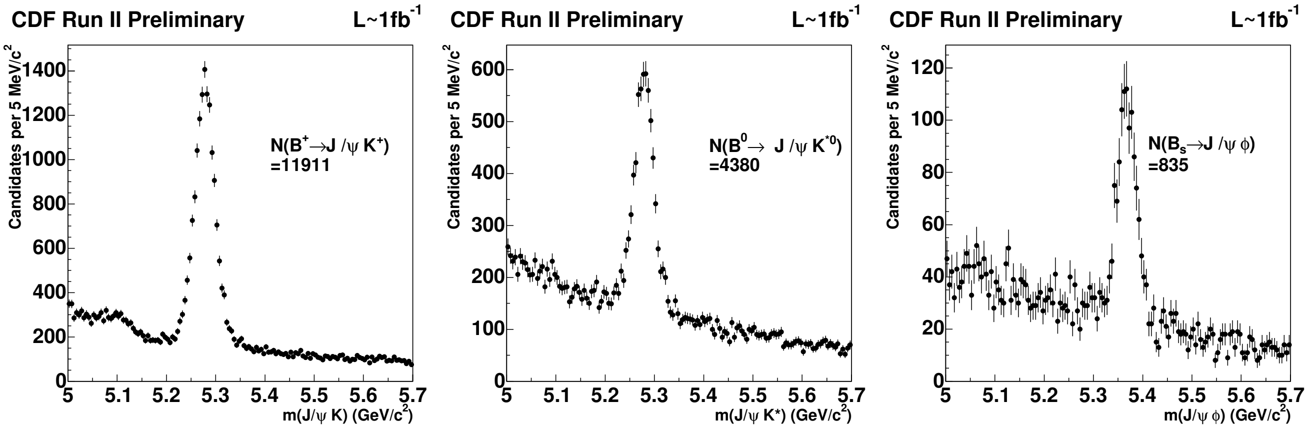

FIG. 1: Yields of the normalization modes with loose selection. The yields are obtained from a fit to a linear background shape and a single Gaussian for the signal.

remaining $\approx 10\%$ has a wider invariant mass distribution. To select the normalization samples, the dimuon invariant mass is required to be within $50\,\mathrm{MeV}/c^2$ of the J/ψ mass. The $B \to J/\psi h$ yields with this loose selection are shown in Figure 1. Fits of a single Gaussian with a linear background result in widths consistent with $20\,\mathrm{MeV}/c^2$ for all three modes.

For the selection of the $B \to \mu^+\mu^- h$ signal, four different vetoes are applied to reduce the peaking backgrounds:

- Candidates with a dimuon mass near the J/ψ and ψ' are rejected: $2.9 \le m(\mu^+\mu^-) \le 3.2\,\mathrm{GeV}/c^2$ and $3.6 \le m(\mu^+\mu^-) \le 3.75\,\mathrm{GeV}/c^2$.
- We reject candidates consistent with originating from a $B \to J/\psi(')h$ decay followed by the decay of the $J/\psi(')$ into two muons and a photon: $|(m_{\mu\mu h} - m_B) - (m_{\mu\mu} - m_{J/\psi(')})| \le 100\,\mathrm{MeV}/c^2$.
- Candidates with an opposite-sign hadron-muon combination (with the muon mass assigned to both particles) within $40\,\mathrm{MeV}/c^2$ of the J/ψ or ψ' mass are rejected. This removes $B \to J/\psi h$ and $B \to \psi' h$ decays where one of the hadrons is misidentified as a muon.
- We reject candidates in which two-track combinations are compatible within $\pm 25\,\mathrm{MeV}/c^2$ with $D^0 \to K^-\pi^+$ decays, or three-track combinations are compatible within $\pm 25\,\mathrm{MeV}/c^2$ with $D^+ \to K^-\pi^+\pi^+$ or $D_s^+ \to K^+K^-\pi^+$ decays. This removes $B \to D\pi$ decays where two hadrons are misidentified as muons.

We tighten the candidate selection to optimize for the smallest uncertainty on the measurement of the $B \to \mu^+\mu^- h$ branching ratios. This is done by finding the selection with the smallest value of $S/\sqrt{S+B}$, where S is the estimate of the expected yield of the rare decays, and B is the expected background.

S is determined from the yield in the normalization modes, rescaled using measured (for B^+, B_d^0) or predicted (for B_s^0) branching ratios of the rare modes, and the relative selection efficiency between the J/ψ modes and the rare modes, as determined from the Monte-Carlo (MC) simulation.

This analysis requires two independent samples for the background estimate: one for the signal optimization and one for the background measurement. Since the low-mass sideband is expected to contain partially reconstructed B decays similar to the signal, we use only the high-mass sidebands. We use the far sideband, $(9-15)\sigma$ above the B mass, for the signal optimization, leaving the near sideband, $(3-9)\sigma$ above the B mass, for a background measurement, unbiased by the optimization. These sidebands are extrapolated to the signal region using the shape of a sample that is enriched in background by inverting the requirement on the vertex quality.

As illustrated in Figures 2 to 4, we find good discriminating power from the following three variables: the proper lifetime significance, ct/σ_{ct}; the pointing angle α from the B meson candidate to the primary vertex, and the isolation, I, defined as the transverse momentum carried by the B meson candidate divided by the transverse momentum of all charged particles in a cone around the direction of the B meson candidate.

Using a full grid scan over 625 different combinations of selection thresholds, we find that the optimal values are very similar between the three modes, and we use the average of the three modes: $ct/\sigma_{ct} \ge 14$, $\alpha \le 0.06$, $I \ge 0.6$.

The mass peaks of the normalization modes after tight selection are shown in Figure 5. The signal yield is obtained from the difference of the number of candidates within $\pm 2\sigma$ of the B mass and the number of candidates in the region $\pm(3-5)\sigma$ from the B mass.

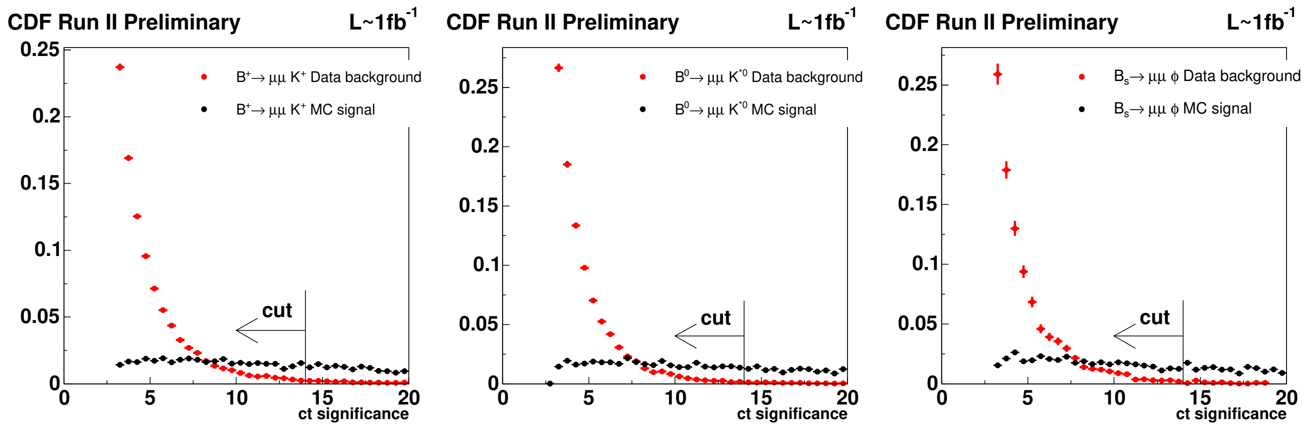

FIG. 2: Comparison between simulated $B \to \mu^+\mu^- h$ signal and $B \to \mu^+\mu^- h$ background from data of the lifetime significance ct/σ_{ct}.

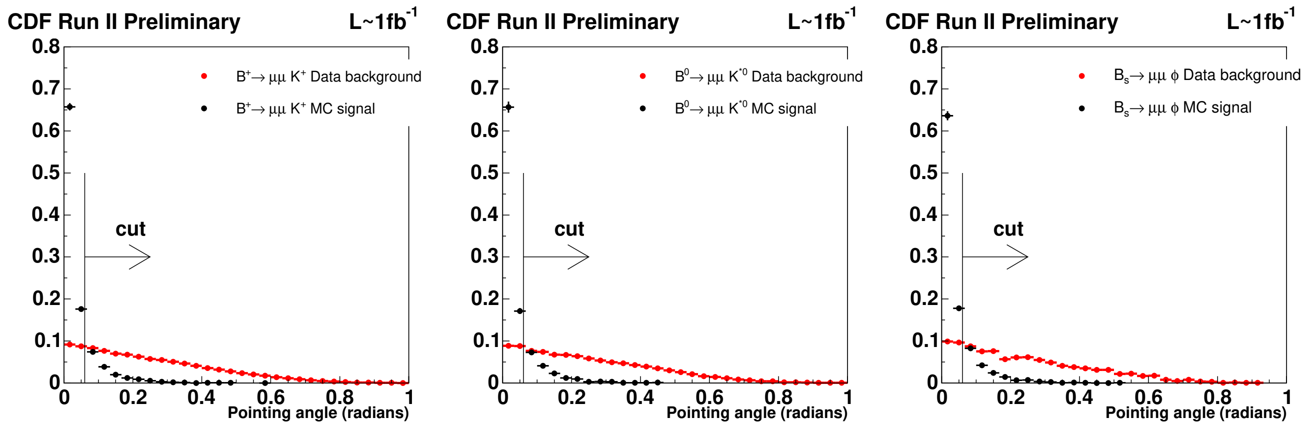

FIG. 3: Comparison between simulated $B \to \mu^+\mu^- h$ signal and $B \to \mu^+\mu^- h$ background from data of the pointing angle α.

Figure 6 illustrates the dependence of the selection efficiency on the dimuon invariant mass. Apart from the vetoes on the J/ψ, ψ', and the D^0, the analysis accepts decays for all allowed values of $m(\mu^+\mu^-)$.

A. Relative efficiency

The selection efficiency for the $B \to \mu^+\mu^- h$ signal is measured relative to the $B \to J/\psi h$ normalization modes using detailed GEANT [12] simulations of both the signal and the normalization modes. The signal modes are generated with the EvtGen package [13], using the models described in References [14, 15]. Since the efficiency for the 4-body decays with a J/ψ in the intermediate state depend on the J/ψ polarization, we generate $B^0_d \to J/\psi K^{*0}$ and $B^0_s \to \mu^+\mu^-\phi$ decays according to the helicity amplitudes measured by CDF [16].

In B^0_s decays, a significant lifetime difference is expected between the light and the heavy mass eigenstates, $\Delta\Gamma/\Gamma = 0.12 \pm 0.06$ [17]. In the decay $B^0_s \to J/\psi\phi$, the short-lived CP-even component dominates [16], and we use a weighted average lifetime of the CP-even and CP-odd lifetimes. For $B^0_s \to \mu^+\mu^-\phi$, we use a central value of 0.5 for the CP-even component, corresponding to the average B_s lifetime.

After reweighing the $p_T(B)$ distribution, we find that the simulation of the normalization modes reproduces the data well, as shown in the Figures 7 to 9. We find relative efficiencies of 0.71 ± 0.01, 0.74 ± 0.02 and 0.84 ± 0.02 respectively for B^+, B^0_d and B^0_s decays, where the errors are from Monte-Carlo statistics only.

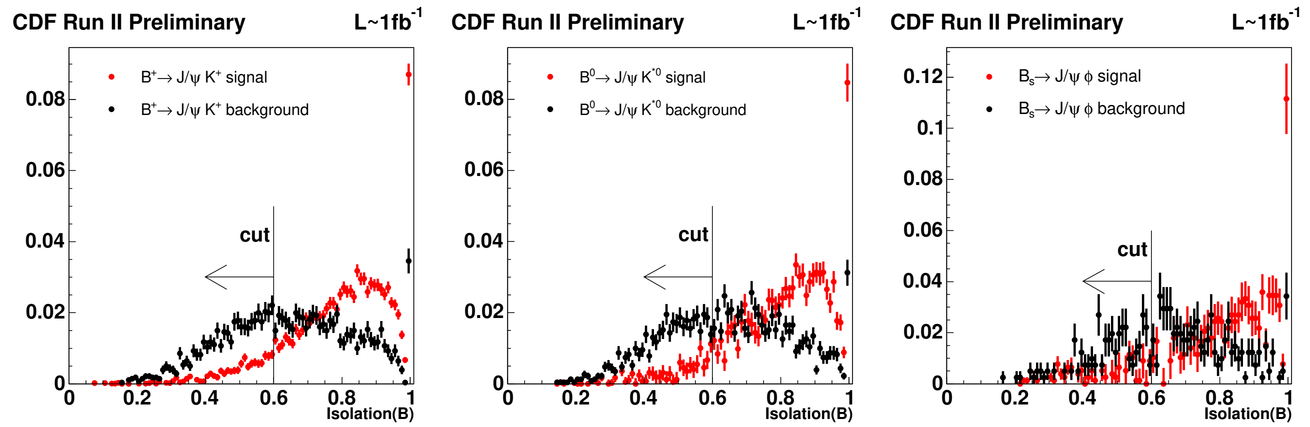

FIG. 4: Comparison between sideband-subtracted $B \to J/\psi h$ signal from data and $B \to \mu^+\mu^- h$ background from data of the isolation variable I.

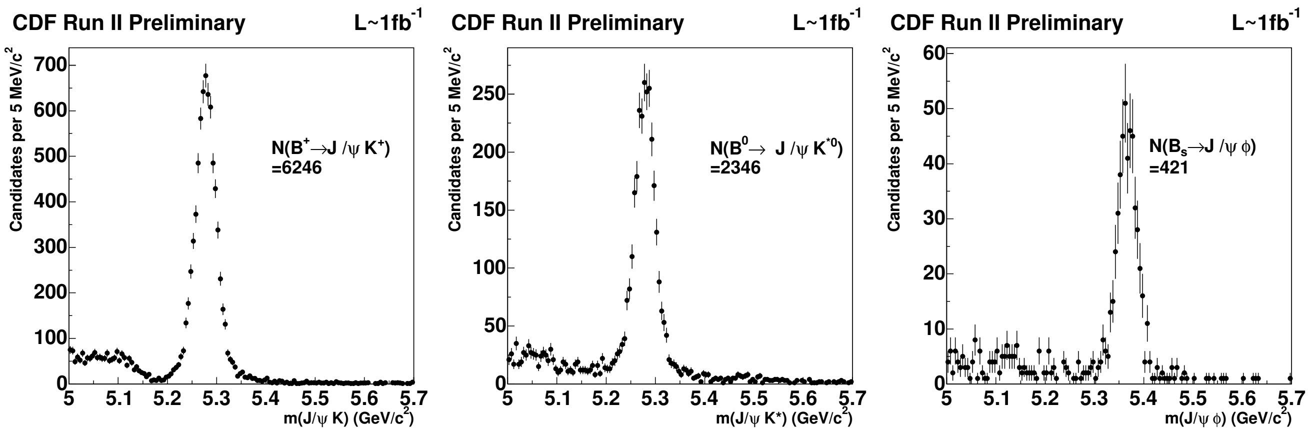

FIG. 5: Yields of the normalization modes with tight selection.

IV. BACKGROUNDS

A. Backgrounds peaking in the signal window

We consider backgrounds peaking in the signal window from the following sources:

- Charmless B decays into charged hadrons, where two charged hadrons are misidentified as muons. We calculate this background from a simulation of charmless B decays, convoluted with the misidentification rates of the

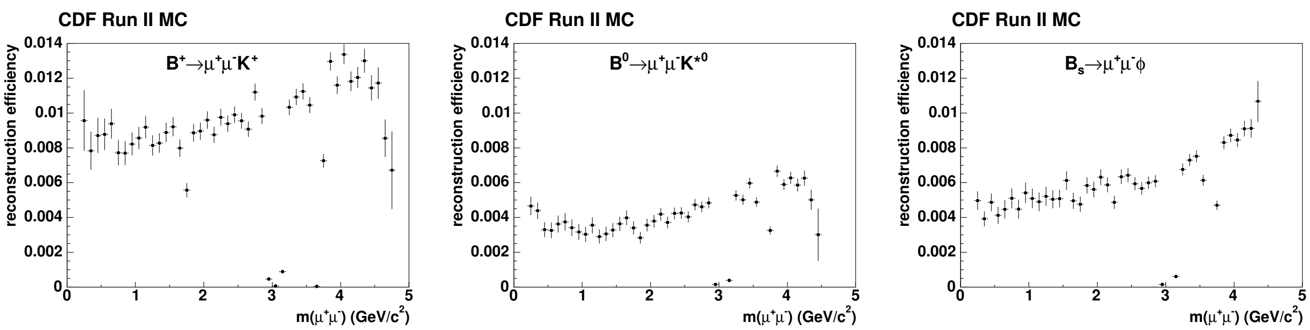

FIG. 6: Dependence of the selection efficiency on the invariant mass of the dimuon system.

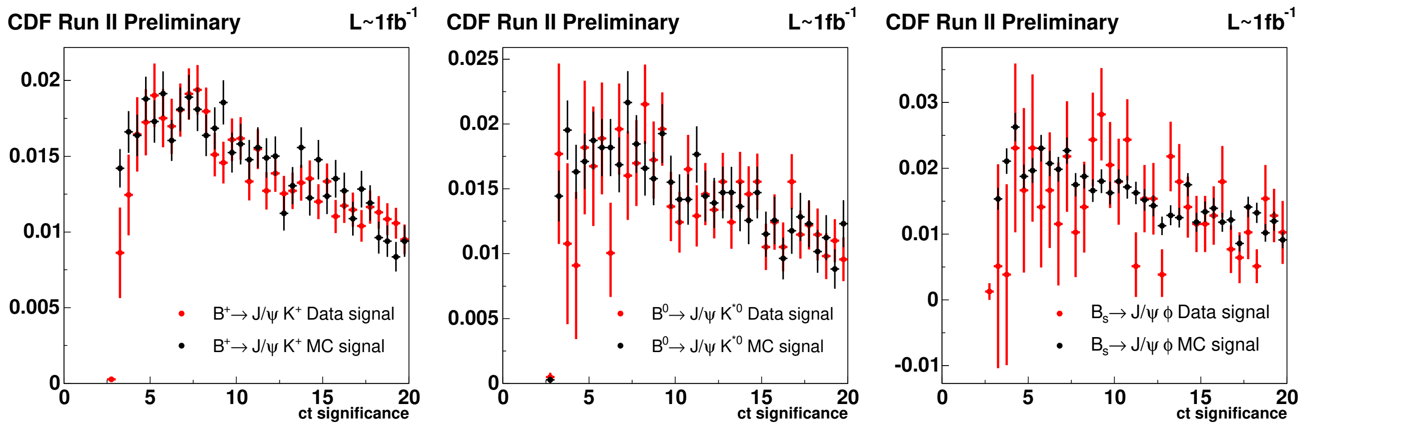

FIG. 7: Data/MC comparison of the lifetime significance ct/σ_{ct}.

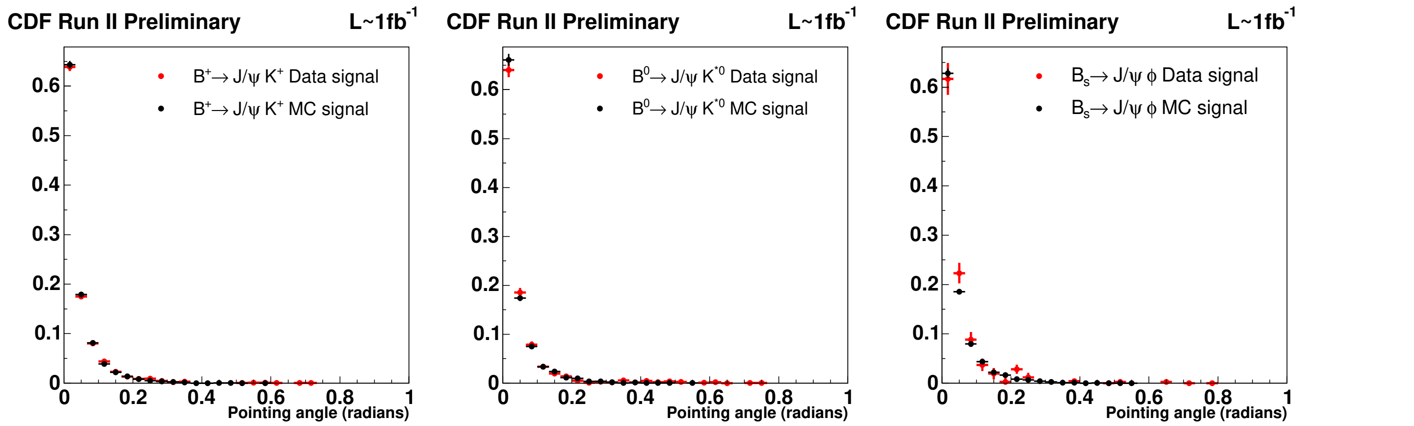

FIG. 8: Data/MC comparison of the pointing angle α.

muon detectors, which are measured in D^*-tagged $D^0 \to K^-\pi^+$ decays. We find a net background of 1.0 events in the $B^+ \to \mu^+\mu^-K^+$ window, dominated by $B^+ \to K^+\pi^-\pi^+$ decays. For the B_d^0 and B_s^0 modes this background is negligible.

- We evaluate reflections between the three rare modes and find a contribution of 0.4 $B_d^0 \to \mu^+\mu^-K^{*0}$ decays reconstructed as $B_s^0 \to \mu^+\mu^-\phi$, and 0.2 $B_s^0 \to \mu^+\mu^-\phi$ decays reconstructed as $B_d^0 \to \mu^+\mu^-K^{*0}$.

B. Continuous background

The continuous background is estimated from the high-mass sidebands, $(3-9)\sigma$ above the B mass, which has not been biased by the optimization of the signal selection. This sideband is extrapolated under the signal region using the background shape from the data distribution with poor vertex quality (χ^2 probability $< 10^{-3}$). As shown in Table I, this is the dominant background for all three modes.

Mode	$B^+ \to \mu^+\mu^-K^+$	$B_d^0 \to \mu^+\mu^-K^{*0}$	$B_s^0 \to \mu^+\mu^-\phi$
Continuous	44.3 ± 5.8	16.3 ± 3.6	3.1 ± 1.5
Peaking BG	1.0	—	—
Cross-talk	—	0.2	0.4
Total	45.3 ± 5.8	16.5 ± 3.6	3.5 ± 1.5

TABLE I: Background prediction in each rare mode.

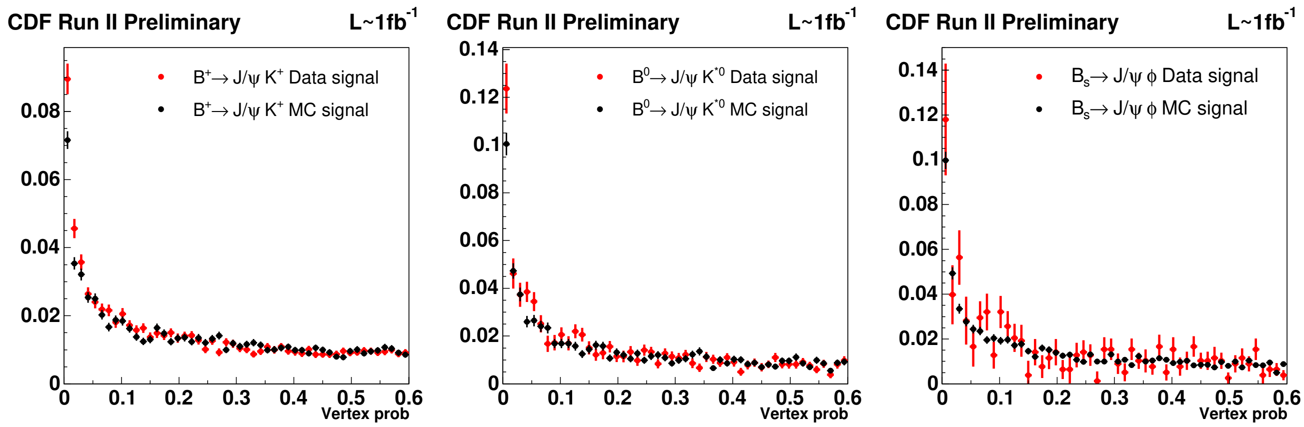

FIG. 9: Data/MC comparison of the χ^2 probability of the vertex fit.

V. SYSTEMATIC UNCERTAINTIES

The following systematic uncertainties have been evaluated:

- The branching ratios of the normalization modes have uncertainties of 4.0%, 5.3%, and 35.5% respectively for B^+, B_d^0, and B_s^0. These uncertainties enter only in the absolute branching ratio measurements.
- The branching ratio of $J/\psi \to \mu^+\mu^-$ has an uncertainty of 1.7%.
- The largest difference in relative efficiency between the default decay model for the rare modes [15] and two alternative models [18, 19] is 3.1% for the B_d^0 and less for the other channels.
- The uncertainty related to the $p_T(B)$ spectrum uncertainty is evaluated from the difference in the relative efficiency with and without the p_T reweighting. The difference is up to 3.8% for the B_d^0, but smaller for the other channels.
- The muon trigger efficiency close to the 1.5 GeV/c threshold is not well known. We find a change in the relative efficiency of up to 1.3% if the threshold is raised to 1.6 GeV/c.
- The signal modes have approximately 10% more low momentum tracks than the normalization modes, and the simulation models the track reconstruction efficiency at small momentum to an accuracy of approximately 2%. We therefore assign a systematic error on the relative efficiency of 2%×10%=0.2%.
- We find an uncertainty of 8.3% on the relative efficiency of B_s^0 decays due to the unknown fraction of short-lived CP-even state in the rare mode. In addition, the uncertainty on $\Delta\Gamma/\Gamma = 0.12 \pm 0.06$ contributes another 2.6%, resulting in a total uncertainty of 8.7% associated with the B_s^0 lifetime difference.
- We evaluate the effect of the unknown fraction of J/ψ produced with a longitudinal polarization by varying its fraction by 1σ. The effect is 0.6% for $B_d^0 \to J/\psi K^{*0}$ and 0.1% for $B_s^0 \to J/\psi\phi$.
- The yields in the normalization modes have associated statistical errors that are included as a systematic error, which ranges from 1.3% for the B^+ channel to 4.8% for the B_s^0.
- Cabibbo-suppressed $B^+ \to J/\psi\pi^+$ decays contribute to the normalization mode of the B^+ channel with a net contribution of 0.1% of the total yield. We do not correct for this small contribution, but instead apply the full effect as a systematic uncertainty.
- The relative efficiencies between the signal and normalization modes are obtained from MC samples of finite statistics, resulting in uncertainties of up to 2.6%.
- The extrapolation of the continuous background from the sideband to the signal region depends on the shape of the background function. We vary the selection of the background-enriched sample from the default inverted-χ^2 vertex selection to one that is similar to the optimal selection, but has less stringent requirements on the three optimization variables. In addition, we evaluate the difference between the default extrapolation and a simpler

Source	$B^+ \to \mu^+\mu^- K^+$	$B_d^0 \to \mu^+\mu^- K^{*0}$	$B_s^0 \to \mu^+\mu^- \phi$
B($B \to J/\psi h$)	4.0	5.3	35.5
B($J/\psi \to \mu^+\mu^-$)	1.7	1.7	1.7
Theory model	1.5	3.1	1.6
$p_T(B)$ spectrum	1.3	3.8	1.2
Trigger turn-on	1.3	1.3	1.2
Low momentum hadrons	0.2	0.2	0.2
B_s^0 lifetime difference	-	-	8.7
Polarization	0	0.6	0.1
Normalization mode statistical error	1.3	2.1	4.8
$B^+ \to J/\psi\pi^+$ Contribution	0.1	-	-
MC statistics $\epsilon_{\mu^+\mu^-}/\epsilon_{J/\psi}$	1.6	2.6	2.2
Background Prediction	5.2	3.1	10.2

TABLE II: Systematic errors as percentage contributions.

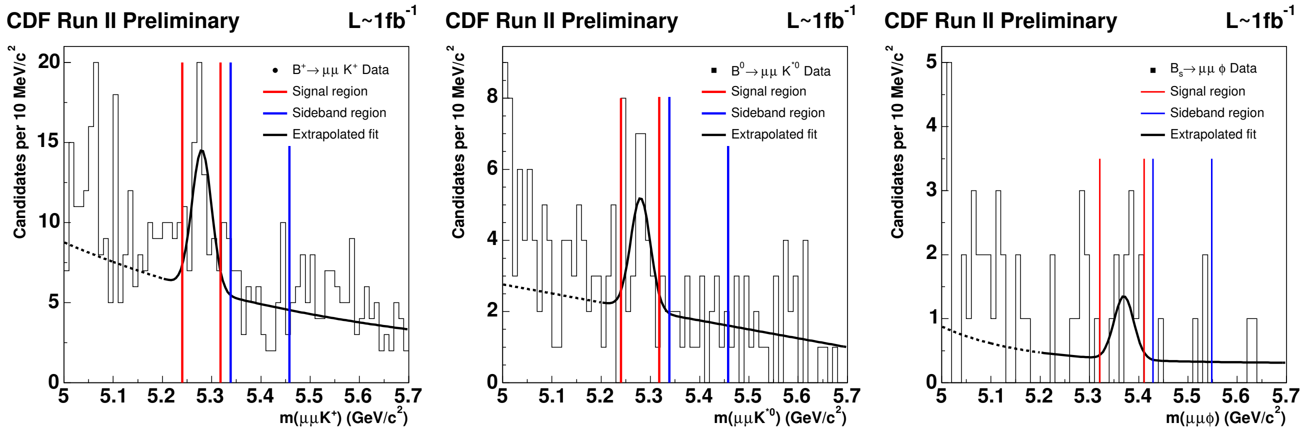

FIG. 10: Invariant mass spectra for the rare modes. The black curves illustrate the expected shape for values measured in the signal and sideband regions: a single Gaussian with a width of 20 MeV/c^2 centered at the B mass for the signal and the sum of an exponential and a constant for the background. Below the B mass, the curve is dotted to indicate that it is not expected to describe the background due to the presence of partially reconstructed B decays.

linear extrapolation. We find a systematic uncertainty on the background prediction of up to 10% for the B_s^0 channel.

All uncertainties are summarized in Table II.

VI. RESULTS

The invariant mass distributions for the signal modes are shown in Figure 10. The candidates in the $\pm 2\sigma$ window around the B mass are listed in Table III. We find an excess in all three modes. Figure 11 shows that the raw distributions of the dimuon invariant mass of the candidates in the three signal regions do not peak at a particular value.

We determine the significance of each excess by calculating the probability for the background to fluctuate into the number of observed events or more, taking into account the uncertainty on the background, and determine the equivalent number of standard deviations of a Gaussian distribution. We find a significance of 4.5, 2.9, and 2.4 standard deviations respectively for the B^+, B_d^0, and B_s^0 modes.

We proceed to calculate branching ratios for the three modes, according to Equation 1. We find $\mathcal{B}(B^+ \to \mu^+\mu^- K^+)/\mathcal{B}(B^+ \to J/\psi K^+) = (0.59 \pm 0.15 \pm 0.03) \times 10^{-3}$, $\mathcal{B}(B_d^0 \to \mu^+\mu^- K^{*0})/\mathcal{B}(B_d^0 \to J/\psi K^{*0}) = (0.62 \pm 0.23 \pm 0.07) \times 10^{-3}$, and $\mathcal{B}(B_s^0 \to \mu^+\mu^-\phi)/\mathcal{B}(B_s^0 \to J/\psi\phi) = (1.24 \pm 0.60 \pm 0.15) \times 10^{-3}$. Using the world-average branching ratios of the normalization modes [5], we find $\mathcal{B}(B^+ \to \mu^+\mu^- K^+) = (0.60 \pm 0.15 \pm 0.04) \times 10^{-6}$, $\mathcal{B}(B_d^0 \to \mu^+\mu^- K^{*0}) = (0.82 \pm 0.31 \pm 0.10) \times 10^{-6}$, and $\mathcal{B}(B_s^0 \to \mu^+\mu^-\phi) = (1.16 \pm 0.56 \pm 0.42) \times 10^{-6}$. Since the

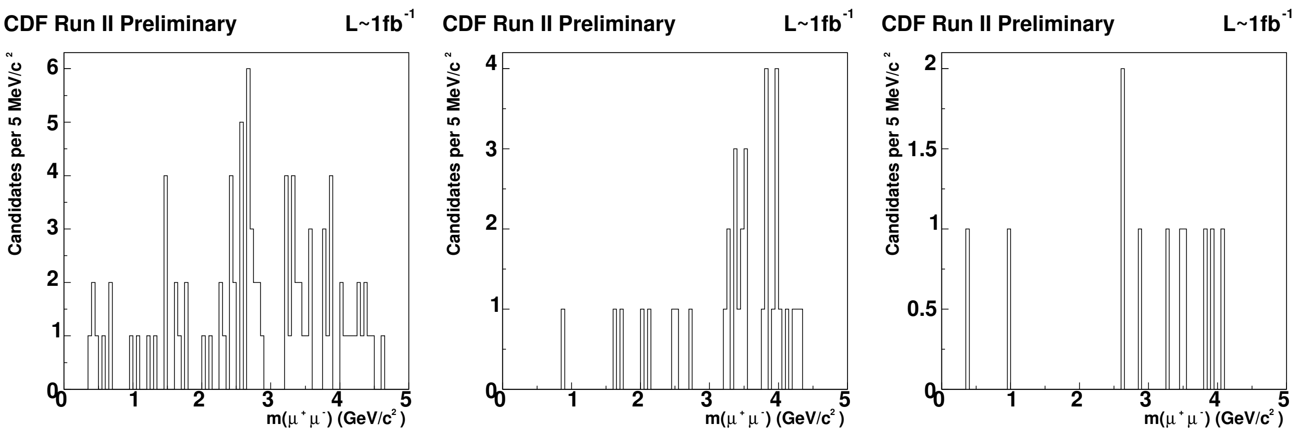

FIG. 11: Raw dimuon invariant mass distributions of the candidates in the signal region.

Mode	$B^+ \to \mu^+\mu^- K^+$	$B_d^0 \to \mu^+\mu^- K^{*0}$	$B_s^0 \to \mu^+\mu^- \phi$
N_S	90	35	11
N_{BG}	45.3 ± 5.8	16.5 ± 3.6	3.5 ± 1.5
Gaussian significance	4.5	2.9	2.4
$N_{J/\psi h}$	6246 ± 79	2346 ± 48	421 ± 21
$\epsilon_{\mu^+\mu^- h}/\epsilon_{J/\psi h}$	0.71 ± 0.01	0.74 ± 0.02	0.84 ± 0.02
Rel $\mathcal{B} \pm stat \pm syst \times 10^{-3}$	$0.59 \pm 0.15 \pm 0.03$	$0.62 \pm 0.23 \pm 0.07$	$1.24 \pm 0.60 \pm 0.15$
Abs $\mathcal{B} \pm stat \pm syst \times 10^{-6}$	$0.60 \pm 0.15 \pm 0.04$	$0.82 \pm 0.31 \pm 0.10$	$1.16 \pm 0.56 \pm 0.42$
Rel $\mathcal{B}$ 95%CL limit $\times 10^{-3}$	—	—	2.61
Rel $\mathcal{B}$ 90%CL limit $\times 10^{-3}$	—	—	2.30

TABLE III: Summary of the main ingredients and results of this analysis.

$B_s^0 \to \mu^+\mu^-\phi$ excess is not significant, we calculate a limit on its relative branching ratio using Bayesian integration assuming a flat prior, and find $\mathcal{B}(B_s^0 \to \mu^+\mu^-\phi)/\mathcal{B}(B_s^0 \to J/\psi\phi) < 2.61(2.30) \times 10^{-3}$ at 95(90)% CL. The main ingredients and the results are summarized in Table III.

In Figure 12 we compare our measurements of the B^+ and B_d^0 modes with previous measurements [6, 20] and find them to be consistent and of similar precision. The limit on the B_s^0 mode is the most stringent to date.

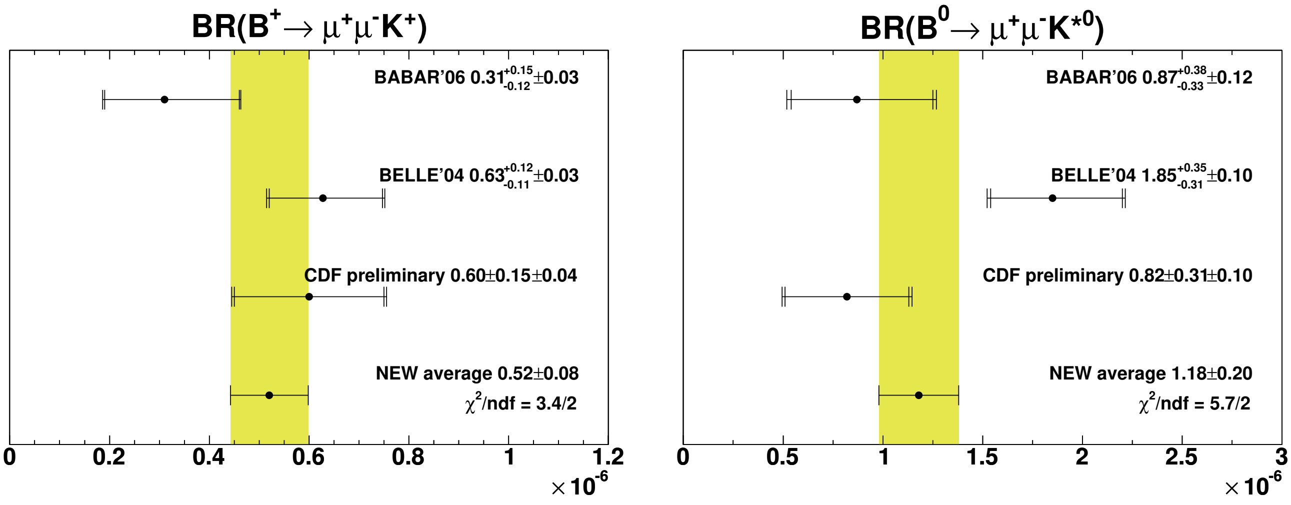

FIG. 12: Comparisons between the present measurements of rare semileptonic B decays and earlier measurements.

Acknowledgments

We thank the Fermilab staff and the technical staffs of the participating institutions for their vital contributions. This work was supported by the U.S. Department of Energy and National Science Foundation; the Italian Istituto Nazionale di Fisica Nucleare; the Ministry of Education, Culture, Sports, Science and Technology of Japan; the Natural Sciences and Engineering Research Council of Canada; the National Science Council of the Republic of China; the Swiss National Science Foundation; the A.P. Sloan Foundation; the Bundesministerium fuer Bildung und Forschung, Germany; the Korean Science and Engineering Foundation and the Korean Research Foundation; the Particle Physics and Astronomy Research Council and the Royal Society, UK; the Russian Foundation for Basic Research; the Comision Interministerial de Ciencia y Tecnologia, Spain; and in part by the European Community's Human Potential Programme under contract HPRN-CT-20002, Probe for New Physics.

---

[1] P. Colangelo, F. De Fazio, R. Ferrandes and T. N. Pham, "Exclusive $B \to K^{(*)}\ell^+\ell^-$, $B \to K^{(*)}\nu\bar{\nu}$, and $B \to K^*\gamma$ transitions in a scenario with a single universal extra dimension," Phys. Rev. D **73**, 115006 (2006) [arXiv:hep-ph/0604029].

[2] F. Kruger and J. Matias, "Probing new physics via the transverse amplitudes of $B_d^0 \to K^{*0}(\to K^-\pi^+)\ell^+\ell^-$ at large recoil," Phys. Rev. D **71**, 094009 (2005) [arXiv:hep-ph/0502060].

[3] T. M. Aliev, A. Ozpineci and M. Savci, "Fourth generation effects in processes induced by $b \to s$ transition," Eur. Phys. J. C **29**, 265 (2003) [arXiv:hep-ph/0301078].

[4] D. A. Demir, K. A. Olive and M. B. Voloshin, "The forward-backward asymmetry of $B \to (\pi, K)\ell^+\ell^-$: Supersymmetry at work," Phys. Rev. D **66**, 034015 (2002) [arXiv:hep-ph/0204119].

[5] W. M. Yao *et al.* [Particle Data Group], "Review of particle physics," J. Phys. G **33** (2006) 1.

[6] B. Aubert *et al.* [BABAR Collaboration], "Measurements of branching fractions, rate asymmetries, and angular distributions in the rare decays $B \to K\ell^+\ell^-$ and $B \to K^*\ell^+\ell^-$," Phys. Rev. D **73**, 092001 (2006) [arXiv:hep-ex/0604007].

[7] A. Ishikawa *et al.* [Belle Collaboration], "Observation of the electroweak penguin decay $B \to K^*\ell^+\ell^-$" Phys. Rev. Lett. **91**, 261601 (2003) [arXiv:hep-ex/0308044].

[8] V. M. Abazov *et al.* [D0 Collaboration], "Search for the rare decay $B_s^0 \to \phi\mu^+\mu^-$ with the D0 detector," Phys. Rev. D **74**, 031107 (2006) [arXiv:hep-ex/0604015].

[9] D. Acosta *et al.* [CDF Collaboration], "Search for the decay $B_s^0 \to \mu^+\mu^-\phi$ in $p\bar{p}$ collisions at $\sqrt{s} = 1.8$ Tev," Phys. Rev. D **65**, 111101 (2002)

[10] C. Q. Geng and C. C. Liu, "Study of $B_s \to (\eta, \eta', \phi)\ell\bar{\ell}$ decays," J. Phys. G **29**, 1103 (2003) [arXiv:hep-ph/0303246].

[11] D. Acosta *et al.* [CDF II Collaboration], "Measurement of the mass difference $m(D_s^+) - m(D^+)$ at CDF II," Phys. Rev. D **68**, 072004 (2003) [arXiv:hep-ex/0310043].

[12] R. Brun *et al.*, "GEANT 3 manual," CERN Program Library Long Writeup W5013, 1994

[13] D. J. Lange, "The EvtGen particle decay simulation package," Nucl. Instrum. Meth. A **462**, 152 (2001).

[14] P. Colangelo, F. De Fazio, P. Santorelli and E. Scrimieri, "QCD Sum Rule Analysis of the Decays $B \to K\ell^+\ell^-$ and $B \to K^*\ell^+\ell^-$," Phys. Rev. D **53**, 3672 (1996) [Erratum-ibid. D **57**, 3186 (1998)] [arXiv:hep-ph/9510403].

[15] A. Ali, P. Ball, L. T. Handoko and G. Hiller, "A comparative study of the decays $B \to (K, K^*)\ell^+\ell^-$ in standard model and supersymmetric theories," Phys. Rev. D **61**, 074024 (2000) [arXiv:hep-ph/9910221].

[16] D. Acosta *et al.* [CDF Collaboration], "Analysis of decay-time dependence of angular distributions in $B_s^0 \to J/\psi\phi$ and $B_d^0 \to J/\psi K^{*0}$ decays and measurement of the lifetime difference between B_s mass eigenstates," Phys. Rev. Lett. **94**, 101803 (2005) [arXiv:hep-ex/0412057].

[17] I. Dunietz, R. Fleischer and U. Nierste, "In pursuit of new physics with B_s decays," Phys. Rev. D **63**, 114015 (2001) [arXiv:hep-ph/0012219].

[18] D. Melikhov and B. Stech, "Weak form factors for heavy meson decays: An update," Phys. Rev. D **62**, 014006 (2000) [arXiv:hep-ph/0001113].

[19] P. Colangelo, F. De Fazio and P. Santorelli, "Form-factor $A_0(q^2)$, nonleptonic $D(B) \to PV$ transitions and rare $B \to K^*\gamma$ decays," Phys. Rev. D **51**, 2237 (1995) [arXiv:hep-ph/9409438].

[20] K. Abe *et al.* [Belle Collaboration], "Measurement of the differential q^2 spectrum and forward-backward asymmetry for $B \to K^*\ell^+\ell^-$" arXiv:hep-ex/0410006.